The free energy is given by

$$\frac{F}{N}=\tfrac{1}{4}(U-2|W|\gamma_0)n^2+\bar{\mu}(n-1)-|W|p^2/\gamma_0 +\frac{1}{N}\sum_{\mathbf{k}}\frac{|\Delta_{\mathbf{k}}|^2}{2E_{\mathbf{k}}}\tanh(\beta E_{\mathbf{k}}/2) -\frac{2}{\beta N}\sum_{\mathbf{k}}\ln[2\cosh(\beta E_{\mathbf{k}}/2)] \ . \qquad (2.15)$$

The pairing potential $V^s_{\mathbf{kq}}$ takes on the separable form in $d=2$ for the square lattice and the nearest-neighbor interaction

$$V^s_{\mathbf{kq}}=-U+\frac{|W|}{4}(\gamma_{\mathbf{k}}\gamma_{\mathbf{q}}+\eta_{\mathbf{k}}\eta_{\mathbf{q}}) +2|W|(\sin k_x\sin q_x+\sin k_y\sin q_y) \ , \qquad (2.16)$$

where $\gamma_{\mathbf{k}}=2(\cos k_x+\cos k_y)$ and $\eta_{\mathbf{k}}=2(\cos k_x-\cos k_y)$. Equation (2.8) can be solved by an ansatz

$$\Delta_{\mathbf{k}}=\Delta_0+\Delta_\gamma\gamma_{\mathbf{k}}+\Delta_\eta\eta_{\mathbf{k}} \ , \qquad (2.17)$$

where the particular terms refer to on-site extended s-wave and d-wave pairing, respectively. The self-consistent equations are

$$\Delta_0=-U\phi_1 \ , \qquad (2.18a)$$

$$\Delta_\gamma=\frac{|W|}{4}\phi_\gamma \qquad (2.18b)$$

for the s-wave pairing, and

$$\Delta_\eta=\tfrac{1}{4}|W|\phi_\eta \qquad (2.18c)$$

for the d-wave pairing.

In Eqs. (2.18a)-(2.18c),

$$\phi_1=\frac{1}{N}\sum_{\mathbf{q}}\Delta_{\mathbf{q}}F_{\mathbf{q}},\ \phi_\gamma=\frac{1}{N}\sum_{\mathbf{q}}\Delta_{\mathbf{q}}\gamma_{\mathbf{q}}F_{\mathbf{q}},\ \phi_\eta=\frac{1}{N}\sum_{\mathbf{q}}\Delta_{\mathbf{q}}\eta_{\mathbf{q}}F_{\mathbf{q}} \ .$$

The transition temperature for the onset of pure s-wave pairing is given by

$$\begin{pmatrix} 1+U\phi_1(T_c) & U\phi_2(T_c) \\ -\frac{|W|}{4}\phi_2(T_c) & 1-\frac{|W|}{4}\phi_\gamma(T_c) \end{pmatrix}\begin{pmatrix}\Delta_0\\ \Delta_\gamma\end{pmatrix}=0 \ , \qquad (2.19a)$$

where

$$\phi_1(T_c)=\frac{1}{N}\sum_{\mathbf{q}}F_{\mathbf{q}}(T_c) \ , \qquad (2.19b)$$

$$\phi_2(T_c)=\frac{1}{N}\sum_{\mathbf{q}}\gamma_{\mathbf{q}}F_{\mathbf{q}}(T_c) \ , \qquad (2.19c)$$

$$\phi_\gamma(T_c)=\frac{1}{N}\sum_{\mathbf{q}}\gamma^2_{\mathbf{q}}F_{\mathbf{q}}(T_c) \ , \qquad (2.19d)$$

and

$$F_{\mathbf{q}}(T_c)=(2\bar{\varepsilon}_{\mathbf{q}})^{-1}\tanh(\beta_c\bar{\varepsilon}_{\mathbf{q}}/2) \ . \qquad (2.20)$$

T_c for the d-wave pairing is

$$\frac{4}{|W|}=\frac{1}{N}\sum_{\mathbf{q}}\eta^2_{\mathbf{q}}F_{\mathbf{q}}(T_c) \ . \qquad (2.21)$$

Notice that the strict separation of the transition temperatures implies that T_c for d-wave pairing is independent of U. An ansatz of the form of Eq. (2.17) amounts to neglecting the relative phases of d- and s-wave order parameters, and hence is not the most general one.[18] Such a phase coupling could be of importance for studying the mixed s-d wave state below T_c.

B. Equal-spin (triplet) pairing

We consider here the case of $|\Delta_t^\uparrow|=|\Delta_t^\downarrow|$ and require $\Delta_t^\uparrow(\mathbf{k})=\Delta_t(\mathbf{k})$, $\Delta_t^\downarrow(\mathbf{k})=\Delta_t^*(\mathbf{k})$.[19] Indeed $\Delta_t(\mathbf{k})=-\Delta_t(-\mathbf{k})$. The self-consistent equation for $\Delta_t(\mathbf{k})$ is

$$\Delta_t(\mathbf{k})=\frac{1}{N}\sum_{\mathbf{q}}V^t_{\mathbf{kq}}\Delta_t(\mathbf{q})F_{\mathbf{q}} \ , \qquad (2.22)$$

where $F_{\mathbf{q}}$ is given by (2.9) and

$$E_{\mathbf{q}}=\sqrt{\bar{\varepsilon}^2_{\mathbf{q}}+|\Delta_t(\mathbf{q})|^2},\ V^t_{\mathbf{kq}}=\tfrac{1}{2}(W_{\mathbf{k+q}}-W_{\mathbf{k-q}}) \ . \qquad (2.23)$$

The equations for p and μ are the same as for the singlet pairing; moreover, the free energy takes on the form of Eq. (2.15) if $\Delta_{\mathbf{k}}$ is replaced by $\Delta_t(\mathbf{k})$. For the $d=2$ square lattice one obtains after substituting $\Delta_t(\mathbf{k})=\Delta^p_x\sin k_x+\Delta^p_y\sin k_y$:

$$\Delta^p_\alpha=\frac{2|W|}{N}\sum_{\mathbf{q}}\sin^2(q_\alpha)\Delta^p_{\mathbf{q}}F_{\mathbf{q}},\ \alpha=x,y \qquad (2.24)$$

with $\Delta\mathbf{q}^p$ having p-like character. T_c for the onset of p-wave pairing is determined by

$$\frac{1}{2|W|}=\frac{1}{N}\sum_{\mathbf{q}}\sin^2(q_x)F_{\mathbf{q}}(T_c) \ , \qquad (2.25)$$

where $F_{\mathbf{q}}(T_c)$ is given by Eq. (2.20).

C. SDW state

The order parameter m_Q is given by

$$m_Q=\frac{Um_Q}{4N}\sum_{\mathbf{q}}\frac{1}{x_{\mathbf{q}}}[\tanh(\beta E^+_{\mathbf{q}}/2)-\tanh(\beta E^-_{\mathbf{q}}/2)] \ . \qquad (2.26)$$

The chemical potential satisfies

$$n-1=-\frac{1}{2N}\sum_{\mathbf{q}}[\tanh(\beta E^+_{\mathbf{q}}/2)+\tanh(\beta E^-_{\mathbf{q}}/2)] \ , \qquad (2.27)$$

where the quasiparticles energies are given by

$$E^\pm_{\mathbf{q}}=\tfrac{1}{2}(\bar{\varepsilon}_{\mathbf{q}}+\bar{\varepsilon}_{\mathbf{q+Q}})\pm x_{\mathbf{q}} \ , \qquad (2.28a)$$

$$x_{\mathbf{q}}=\sqrt{\tfrac{1}{4}(\bar{\varepsilon}_{\mathbf{q}}-\bar{\varepsilon}_{\mathbf{q+Q}})^2+U^2m^2_Q} \ , \qquad (2.28b)$$

and $\bar{\varepsilon}_{\mathbf{q}}=\varepsilon_{\mathbf{q}}+p|W||\gamma_{\mathbf{q}}|/\gamma_0-\bar{\mu}$. The Fock parameter satisfies the equation

$$p=-\frac{1}{2N}\sum_{\mathbf{q}}\gamma_{\mathbf{q}}[\tanh(\beta E^+_{\mathbf{q}}/2)+\tanh(\beta E^-_{\mathbf{q}}/2)] +\frac{1}{4N}\sum_{\mathbf{q}}\frac{\gamma_{\mathbf{q}}(\bar{\varepsilon}_{\mathbf{q}}-\bar{\varepsilon}_{\mathbf{q+Q}})}{x_{\mathbf{q}}}[\tanh(\beta E^-_{\mathbf{q}}/2) -\tanh(\beta E^+_{\mathbf{q}}/2)] \ . \qquad (2.29)$$

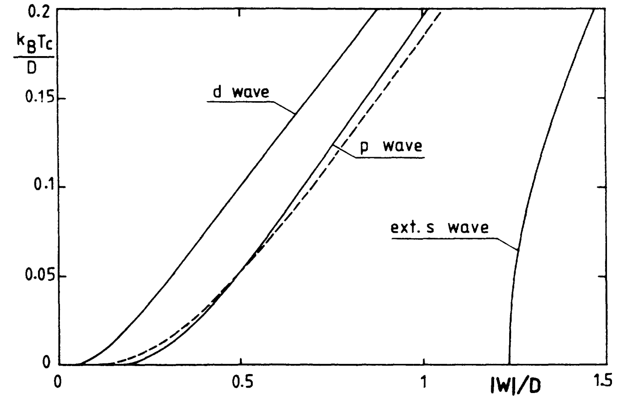

FIG. 1. T_c for *d*-, *p*-, and extended *s*-wave pairings for the square lattice and half-filled band. The dashed line indicates T_c for both on-site (s) pairing vs $-U/D$ and SDW vs U/D.

For the half-filled-band case we have also checked the sensitivity of T_c for the *s*-wave pairing with respect to the different choices of the DOS. For the $U<0$ Hubbard model the on-site *s*-wave pairing is strongly enhanced by Van Hove's singularity in comparison to the square DOS. On the other hand, the extended *s*-wave pairing for $W<0$ is overestimated by the square DOS in comparison to the exact one.

Let us now come to the case of arbitrary band filling. For $n \neq 1$ one has to solve the equations for T_c (2.19)–(2.21) and (2.25) together with the equation fixing the chemical potential, which is given by

$$n-1=-\frac{2}{N}\sum_{\mathbf{q}}\bar{\varepsilon}_{\mathbf{q}}F_{\mathbf{q}}(T_c)\ , \tag{3.7}$$

with $\bar{\varepsilon}_{\mathbf{q}}=\varepsilon_{\mathbf{q}}-\bar{\mu}$, and $F_{\mathbf{q}}(T_c)$ given by Eq. (2.20).

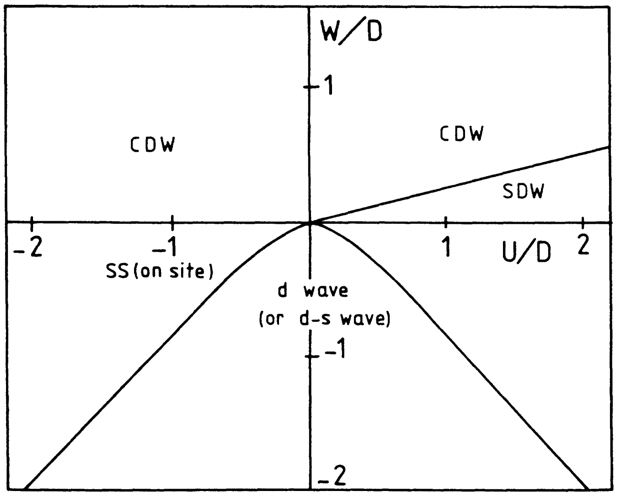

FIG. 2. A preliminary ground-state phase diagram of the extended Hubbard model in two dimensions and square lattice for $n=1$. CDW denotes charge-density waves; SDW denotes spin-density waves; SS denotes singlet pairing (on-site). *d*-*s* means a possible mixed superconducting state of *d*-wave and *s*-wave admixture.

Consider first of all the *s*-wave pairing. Equation (2.19) can be analyzed analytically for arbitrary electron density upon making use of the approximated square DOS

$$\rho(\varepsilon)=\begin{cases}1/2D, & |\varepsilon|\le D\ ,\\ 0, & \text{otherwise}\ .\end{cases} \tag{3.8}$$

Although this DOS neglects the logarithmic singularity it is useful for qualitative analysis. One obtains in the weak-coupling limit (low T_c)

$$k_B T_c=1.14D\sqrt{n(2-n)}\exp\left(-\frac{1+\lambda[3(n-1)^2-1]+\alpha\lambda(n-1)^2}{2\lambda\{(n-1)^2-\alpha/4\lambda+(\alpha/4)[1+(n-1)^2]\}}\right)\ , \tag{3.9}$$

where $\alpha=U/D$ and $\lambda=|W|/D$. To derive (3.9) we have used $\bar{\mu}\approx D(n-1)$ at low T. Equation (3.9) shows, among others, that the s pairing takes place in the whole Brillouin zone with the half-bandwidth playing the role of the energy scale. Moreover Eq. (3.9) indicates that for $U>0$ there exists some limiting value for U and $|W|$ and given density n in order for *s*-wave pairing to exist. The behavior of T_c vs n is nonmonotonous.

For other types of pairing the above approximation based on DOS (3.8) is no longer useful. In general, one can perform the high-T_c expansion for arbitrary value of n to determine T_c for *s*-, *p*-, and *d*-wave pairing in the strong-coupling regime. The weak-coupling formulas for the different pairings with the use of exact DOS or logarithmic approximation and exploring the idea of averaging the pairing potential over the Fermi surface are not accurate, since in our model we essentially allow for pairing in the whole Brillouin zone and there is no cutoff wave vector (except for a reciprocal vector).

The coupled equations for T_c and μ were solved by direct numerical integration, thus properly taking into account the Van Hove singularity. In evaluating T_c for *d*-wave pairing the following exact relation has been used:

$$\phi_\eta=16(\phi_1-\phi_p)-\phi_\gamma\ , \tag{3.10}$$

where

$$\phi_p=\frac{1}{N}\sum_{\mathbf{q}}\sin^2(q_x)F_{\mathbf{q}}(T_c)\ , \tag{3.11}$$

$$\phi_\eta=\frac{1}{N}\sum_{\mathbf{q}}\eta_{\mathbf{q}}^2F_{\mathbf{q}}(T_c)\ , \tag{3.12}$$

which holds for the square lattice, and $\phi_1(T_c)$ and $\phi_\gamma(T_c)$ are given by Eqs. (2.19b) and (2.19d), respectively.

Figures 3–6 gives T_c vs n for different values of U/D and $|W|/D$. These plots are symmetric with respect to $n \rightarrow 2-n$, due to the electron-hole symmetry. For small

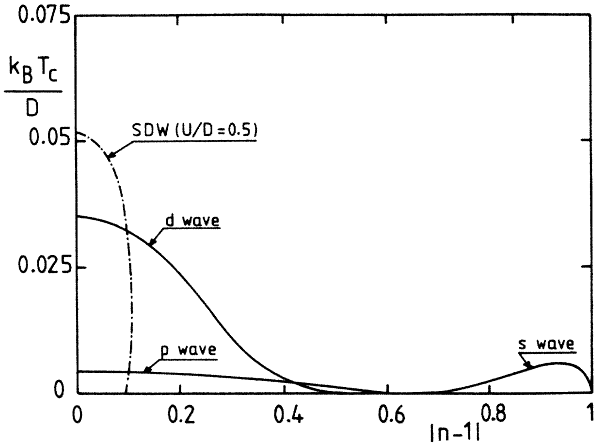

FIG. 3. T_c for *s*-, *p*-, and *d*-wave pairings for the square lattice vs electron density for $|W|/D = 0.25$, $u = 0$. T_c for SDW is marked by the dashed-dot line.

$|W|/D$ the *d*-wave pairing gives high transition temperatures in comparison with the *p*-wave or the extended-*s*-wave pairing. This is related to the fact of a very fast increase of T_c for *d*-wave pairing for small $|W|/D$ (compare Fig. 1). Figure 3 shows the phase diagram for $|W|/D = 0.25$. With increasing $|W|/D$ the other pairings develop and extend their stability regions (Figs. 4-6). For the nearly-half-filled band the *d*-wave pairing always yields the highest T_c, while upon decreasing n the *p*-wave and the *s*-wave pairings become more stable. T_c for both *d* and *p* pairings monotonously decreases with n deviating from $n = 1$. T_c for the *s*-wave pairing exhibits strong nonmonotonic behavior with increasing band filling. It rises rapidly for small n, goes through a maximum, and then vanishes asymptotically below some values of n (Figs. 4 and 5). For $U > 0$, *s* pairing is reduced and the maximum of T_c is shifted towards higher values of $|n-1|$ with increasing U. Let us point out that such a behavior of T_c for the extended *s*-wave pairing is obtained for any $U > 0$ as long as $|W| < |W|_{\text{crit}} = (\pi^2/8)D$. For $|W| > |W|_{\text{crit}}$, T_c tends to a finite value for $n = 1$ (Fig. 5). Moreover, for $U < 0$, the *s*-wave pairing can always be the most stable one for sufficiently large values of negative U. The boundary between the *p*- and *d*-wave pairing states (Fig. 6) is located at $0.2 < n < 0.52$ for $0 < |W|/D \leq 2$. The numerical analysis also indicates that the effect of Van Hove's singularity in DOS is less pronounced with n going toward lower densities, i.e., higher values of $|n-1|$. This is, in particular, observed for on-site *s* pairing and large

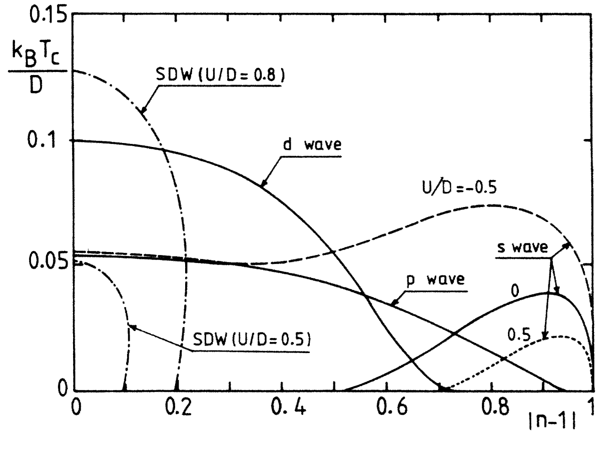

FIG. 4. As in Fig. 3 for $|W|/D = 0.5$ and for different values of U/D.

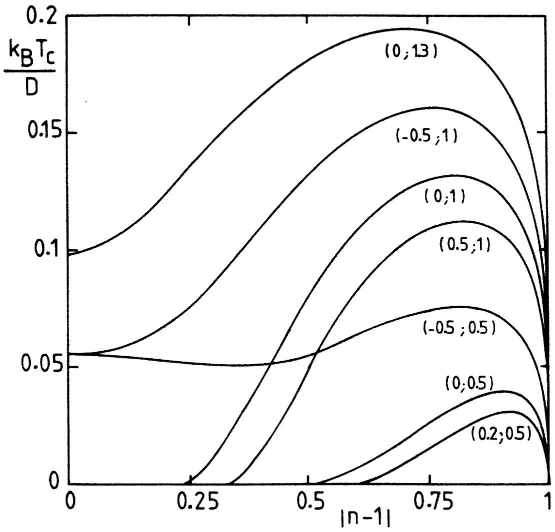

FIG. 5. T_c for *s*-wave pairing vs electron density for different values of $|W|/D$ and U/D. Numbers next to curves are $(U/D; |W|/D)$.

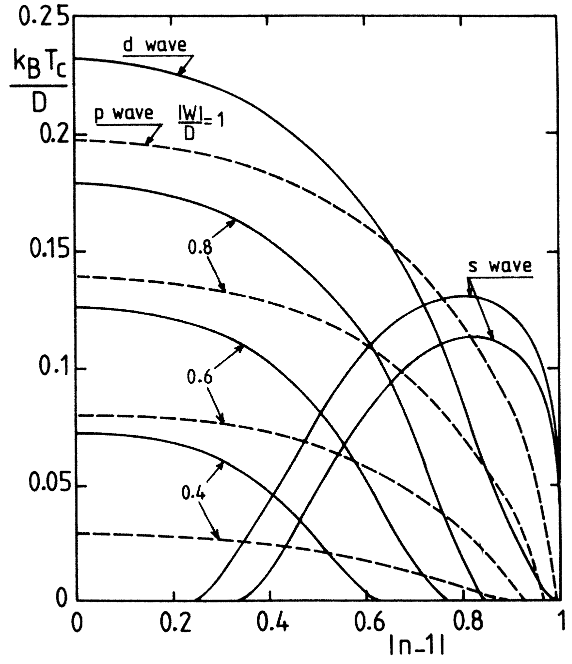

FIG. 6. T_c for *d*- and *p*-wave pairings for several values of $|W|/D$. T_c for *s*-wave pairing: upper curve, $|W|/D = 1.0$ and $U/D = 0$; lower curve, $|W|/D = 1$ and $U/D = 0.5$.

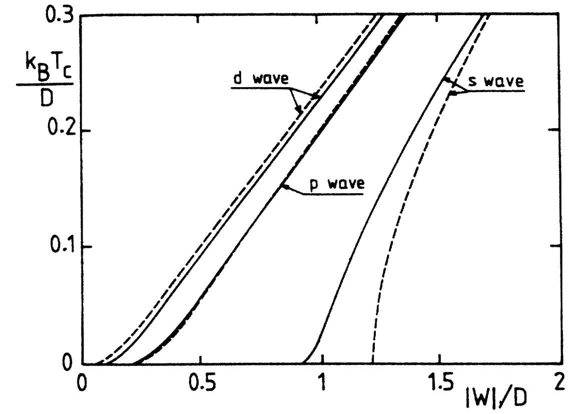

FIG. 7. T_c for d-, p-, and s-wave pairings for $n=1$ for the square lattice with nearest- and next-nearest-neighbor hopping. $t_2/t=0.3$. The dashed lines indicate T_c for $t_2=0$. T_c for p-wave pairing is almost unaltered for this value of t_2/t.

which links the cases of $t_2>0$ and $t_2<0$. In Fig. 8 we compare T_c vs n for $t_2/t=0.3$ with that for $t_2=0$.

The evolution of T_c with increasing t_2/t ratio is clearly indicated by plots in Figs. 8 and 9(a)–9(c). Upon increasing t_2/t the s-wave pairing is enhanced in the regime $1<n<2$ and spread over a wider region of densities. The nonmonotonic variation of T_c with electron density is smoothened upon increasing t_2, and the maximum of T_c moves toward the half-filled band. For $0<n<1$, the s-wave pairing is much reduced upon increasing t_2, but it can still be stable for small n. The effect of $U>0$ on s-wave pairing is illustrated in Fig. 9(a), which shows a reduction of T_c and the movement of the maximum towards lower densities.

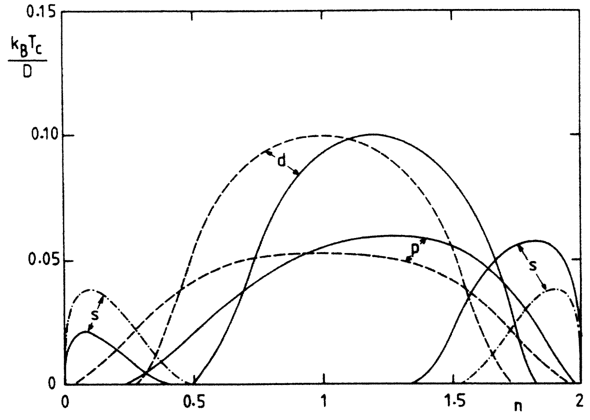

FIG. 8. Comparison of critical temperatures for different types of pairings for the square lattice (for $|W|/D=0.5$, $U=0$) vs electron density with nearest- and next-nearest-neighbor hopping. The solid lines are plotted for $t_2/t=0.3$; the dashed and dashed-dot lines are for $t_2=0$.

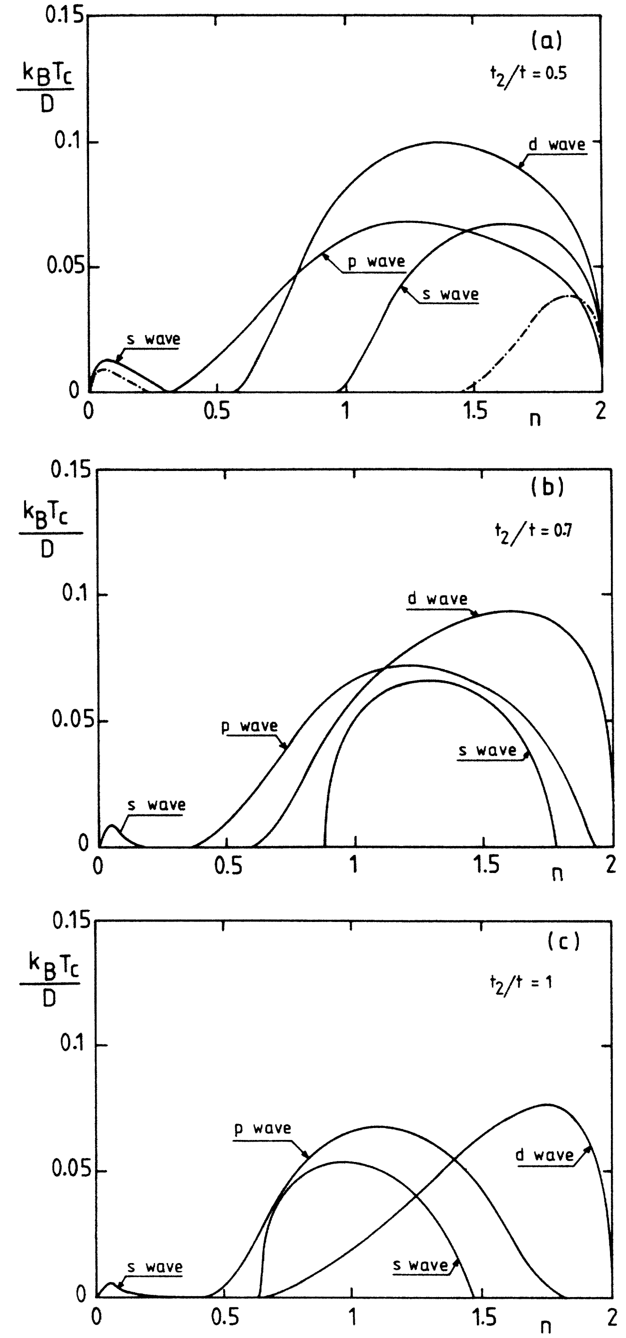

FIG. 9. T_c for d-, p-, and s-wave pairing for the square lattice vs electron density and different ratio t_2/t, for $|W|/D=0.5$, $U=0$. (a) $t_2/t=0.5$; (b) $t_2/t=0.7$; (c) $t_2/t=1.0$. In (a) dashed-dot lines mark T_c for s-wave pairing for $|W|/D=0.5$ and $U/D=0.5$.

The plots for the d-wave pairing are particularly interesting. A maximum of T_c decreases and moves from $n=1$ towards lower densities, and the strong nonmonotonic variation of T_c vs n is observed for a larger t_2/t ratio. As far as the p-wave is concerned, T_c first increases for small t_2/t then its stability range shrinks and the maximum of T_c goes to $n\cong 1$.

From comparison of T_c we give the diagram of relative stability of s-, p-, and d-wave pairings in Fig. 10. One then concludes that the d-wave pairing is the one which is most stable for $1<n<2$ with increasing t_2/t, followed by

dle and several proposals have recently appeared.[10,18,32–35] A rather simplified picture of the superconductivity is obtained upon relaxing the doubly occupancy condition by linearization of the kinetic-energy term $t_{ij}h_{i\sigma}^{\dagger}h_{j\sigma} \rightarrow \delta t_{ij}c_{i\sigma}^{\dagger}c_{i\sigma}$, where $\delta = 1-n$ means the fractional occupation. Such a procedure requires a supplementary projection operation which excludes the doubly occupied sites. We notice that all the mean-field schemes so far proposed in the literature[18,32–35] are internally inconsistent in the limit $\delta = 0$. In this section we propose a simplified but internally consistent mean-field treatment by scaling the spin and charge couplings in the following way, replacing (5.1) by

$$H \cong \sum_{ij\sigma} t_{ij}\delta c_{i\sigma}^{\dagger}c_{j\sigma} + \sum_{ij} J_{ij}\mathbf{S}_i\cdot\mathbf{S}_j + \sum_{ij}\delta W'_{ij}n_in_j - \mu\sum_{i\sigma}n_{i\sigma} + \text{const} \;, \tag{5.3}$$

where

$$W'_{ij} = -\tfrac{1}{4}J_{ij} + \tfrac{1}{2}W_{ij}, \quad n_i = n_{i\uparrow} + n_{i\downarrow} \;.$$

Upon making the Gorkov-type factorizations, we obtain the following gap equation for the singlet pairing (neglecting the Fock averages):

$$\Delta_k = \frac{1}{N}\sum_{\mathbf{q}} V_{\mathbf{kq}}\Delta_{\mathbf{q}}F_{\mathbf{q}} \;, \tag{5.4}$$

where

$$F_{\mathbf{q}} = (2E_{\mathbf{q}})^{-1}\tanh(\beta E_{\mathbf{q}}/2) \;, \tag{5.5}$$

$$E_{\mathbf{k}} = \sqrt{\xi_{\mathbf{k}}^2 + |\Delta_{\mathbf{k}}|^2} \;, \tag{5.6}$$

where

$$\begin{gathered} \xi_{\mathbf{k}} = -t\delta\gamma_{\mathbf{k}} - \mu \text{ and } \gamma_{\mathbf{k}} = 2(\cos k_x + \cos k_y) \;, \\ V_{\mathbf{kq}} = \tfrac{3}{2}J\gamma_{\mathbf{k}-\mathbf{q}} + \tfrac{1}{2}J\delta\gamma_{\mathbf{k}-\mathbf{q}} - W\delta\gamma_{\mathbf{k}-\mathbf{q}} \;. \end{gathered} \tag{5.7}$$

Upon using the decomposition $\Delta_{\mathbf{k}} = \Delta_\gamma\gamma_{\mathbf{k}} + \Delta_\eta\eta_{\mathbf{k}}$ we have respectively for the extended s-wave pairing

$$\Delta_\gamma = \frac{1}{N}\sum_{\mathbf{q}}\tfrac{1}{4}[\tfrac{3}{2}J(1+\delta/3) - W\delta]\gamma_{\mathbf{q}}^2\Delta_{\mathbf{q}}F_{\mathbf{q}} \;, \tag{5.8a}$$

and for the d-wave pairing

$$\Delta_\eta = \frac{1}{N}\sum_{\mathbf{q}}\tfrac{1}{4}[\tfrac{3}{2}J(1+\delta/3) - W\delta]\eta_{\mathbf{q}}^2\Delta_{\mathbf{q}}F_{\mathbf{q}} \;. \tag{5.8b}$$

The chemical potential is determined by

$$\delta = \frac{1}{N}\sum_{\mathbf{q}} 2\xi_{\mathbf{q}}F_{\mathbf{q}} \;. \tag{5.9}$$

We stress that in the present treatment there is no electron-hole symmetry (due to the fact that we work in the lower Hubbard subband) in contrast to the case of the weak electron correlations considered in Sec. III. The transition temperatures for the onset of s- and d-wave pairings is given by

$$\frac{1}{G} = \frac{1}{N}\sum_{\mathbf{q}}\gamma_{\mathbf{q}}^2\frac{\tanh(\beta_c\xi_{\mathbf{q}}/2)}{2\xi_{\mathbf{q}}} = \phi_\gamma(T_c) \;, \tag{5.10a}$$

$$\frac{1}{G} = \frac{1}{N}\sum_{\mathbf{q}}\eta_{\mathbf{q}}^2\frac{\tanh(\beta_c\xi_{\mathbf{q}}/2)}{2\xi_{\mathbf{q}}} = \phi_\eta(T_c) \;, \tag{5.10b}$$

$$G = \tfrac{3}{8}J(1+\delta/3) - \tfrac{1}{4}W\delta \;, \tag{5.10c}$$

and μ is given by Eq. (5.9) for $\Delta \rightarrow 0$. Had we worked with the Hamiltonian (5.3) without rescaling W' [by setting $\delta = 1$ in Eqs. (5.7) and (5.10c)] we would have obtained a T_c dependent on W even in the half-filled-band case where we have no charge coupling in (5.1). With our proposed scaling of this term we find for $\delta \rightarrow 0$, $k_BT_c = \frac{3}{8}J$ for both types of couplings and hence no inconsistencies at least on this level of a mean-field approach. The fact that one obtains a finite T_c for $n = 1$ is an artifact of the mean-field result (i) due to the neglect of phase fluctuations and (ii) due to not projecting out the doubly occupied states (see, however, Refs. 10 and 35). It is expected that a proper mean-field treatment should lead to the physical order parameter $\tilde{\Delta} = \Delta\delta$ which naturally vanishes for $n = 1$.

It is interesting to observe that for small deviations from $n = 1$, the d-wave state gives the highest T_c. This can be shown by making use of strong-coupling expansion (high T_c) of ϕ_γ and ϕ_η. One has for $d = 2$,

$$\phi_\gamma(T_c) = \beta_c\left[1 - \frac{(\beta_c\mu)^2}{12} - \tfrac{3}{4}(\beta_ct\delta)^2 + \cdots\right] \;, \tag{5.11a}$$

$$\phi_\eta(T_c) = \beta_c\left[1 - \frac{(\beta_c\mu)^2}{12} - \frac{(\beta_ct\delta)^2}{12} + \cdots\right] \;. \tag{5.11b}$$

Since in the lowest order $\beta_c\mu \approx 2\delta$ one gets for T_c^s and T_c^d, respectively,

$$k_BT_c^s = G\left[1 - \frac{\delta^2}{3} - \frac{3t^2\delta^2}{4G^2} + \cdots\right] \;, \tag{5.12a}$$

$$k_BT_c^d = G\left[1 - \frac{\delta^2}{3} - \frac{t^2\delta^2}{12G^2} + \cdots\right] \;, \tag{5.12b}$$

which shows that the T_c for s-wave pairing is always less than for the d-wave pairing, and indeed any $W < 0$ strongly stabilizes the superconducting state.

As far as the p-wave (equal spin) pairing is concerned, it can only result from the W term, since the equal spin contribution precisely cancels in the second term of (5.1). The gap equation is formally given by our previous equation (2.22) with that difference that now the pairing potential is $V_{kq}^{\dagger} = \frac{1}{2}(W_{k+q} - W_{k-q})$. δ and $\bar{\varepsilon}_q = \xi_q = -t\delta\gamma_q - \mu$. T_c for the p-wave pairing is then given by [compare Eq. (2.25)]

$$1 = \frac{2|W|\delta}{N}\sum_{\mathbf{q}}\sin^2 q_x\frac{\tanh(\beta_c\xi_{\mathbf{q}}/2)}{2\xi_{\mathbf{q}}} = 2|W|\delta\phi_p(T_c) \;. \tag{5.13}$$

Upon making the high-temperature expansion we obtain for $d = 2$,

$$\phi_p(T_c) = \frac{\beta_c}{8}\left[1 - \frac{(\beta_c\mu)^2}{12} - \frac{(\beta_ct\delta)^2}{4} + \cdots\right] , \tag{5.14}$$

which in lowest order of approximation yields

$$k_BT_c^p \cong \frac{|W|\delta}{4}\left[1 - \frac{\delta^2}{3} - 4t^2/W^2 + \cdots\right] \;. \tag{5.15}$$

This shows that T_c^p starts from the origin as a function of doping. If we had not scaled the pairing potential by δ then the result would have been

$$k_B T_c^p \cong \frac{|W|}{4}\left[1-\frac{\delta^2}{3}-\frac{4t^2\delta^2}{W^2}+\cdots\right], \quad (5.16)$$

giving finite T_c for $\delta=0$.

A detailed discussion of the phase diagram in the $U \gg t$ limit for anisotropic superconductivity would require numerical work on the above set of equations. Moreover, the inclusion of pair hopping terms (not considered here) will stabilize the extended s-wave pairing. An entirely different approach to the strong correlations ($U \gg t$) problem close to the half-filled-band case is to consider the possibility of the formation and condensation of charged bosons—either local pairs of holes or bosons resulting from the RVB state.[10,12,32,35] These challenging problems are presently under investigation.

VI. DISCUSSION

In this paper we have carried out the mean-field analyses of the superconductivity in a narrow-band system with local short-range attractive interactions for two dimensions and arbitrary band filling. Based on the extended Hubbard model with nearest-neighbor attractive interaction we determined the superconducting transition temperatures for singlet pairings of d and s type and for equal-spin, triplet pairing which is of p type, as well as the SDW state. Our analysis in the case of nearest-neighbor hopping shows that close to the half-filled band d-wave pairing is most stable, while the p wave is stabilized for intermediate densities. T_c for s-wave pairing showing a strong nonmonotonous behavior as a function of electron densities is essentially realized for small densities, and is most affected by the on-site repulsion. In principle, one then expects the following order of transitions with increasing electron density: $s \rightarrow p \rightarrow d$ wave. This has to be compared, however, on the mean-field level with the SDW state which is realized close to $n=1$ and can be always most stable for sufficiently large $U>0$. It is interesting to compare the superconducting phases for $W<0$ with that of a purely attractive Hubbard model. For the $U<0$ Hubbard model, T_c for on-site pairing shows smooth behavior versus electron density and is always enhanced by the Van Hove singularity in $d=2$ for the square lattice. This pairing exists for any $U<0$ and arbitrary n. In the case of intersite attraction, we observe for s-wave pairing a sharp rise of T_c for small densities, then a maximum, and finally T_c vanishing asymptotically below some density. Moreover, for the $U<0$ Hubbard model one can go continuously to the large attraction limit, i.e., from the Cooper pairs to the local pairs.[7,21,22] For $W<0$ it is an open question of whether one can reach the limit of local intersite pairs by continuing from the Hartree-Fock limit.

In the case of next-nearest-neighbor hopping we observed essential changes in the phase diagrams with varying electron densities. This can be of importance as far as the T_c dependence on pressure is concerned. We did not consider the role of the Fock terms, which we believe changes only quantitatively the picture with the mean-field theory and leads essentially to temperature renormalization of the bandwidth. We discussed the SDW instability, which for the strictly $d=2$ system indicates only the presence of spin fluctuations but not a real phase transition. A coexistence of the SDW and anisotropic superconductivity is an interesting problem which is left for a future study.

The question of condensation transition for attractive interaction should also be addressed as far as the thermodynamic properties of the extended Hubbard model is concerned. In this respect we should only mention that for real systems long-range Coulomb interactions will have to be taken into account, which always will lead to the suppression of the condensed state. The applicability of the mean-field theory for strictly two-dimensional systems cannot be resolved unless the fluctuations are considered. This certainty calls for theories beyond RPA or renormalization-group studies.

For $U \gg t$, we demonstrated that our model is close to recent proposals for mechanism for high T_c superconductivity, with that difference that in our model superconductivity is an intrinsic consequence of the attractive intersite interaction. We should also stress the difference between the limits of weak and strong correlations. In the limit of weak correlations the anisotropic superconductivity can be readily established even for $n \approx 1$. In contrast for $U \gg t$ limit, the localization effects are important, and for $n=1$, certainly any superconductivity is absent. It is a very interesting question whether one can have the formation of real-space pairs for small electron densities and intersite attractive interaction. Our previous studies of the local-pair superconductivity restricted to effective on-site pairs indicate that a system of tightly bound pairs can undergo the Bose-condensation and this may lead to a superconductivity of a hard-core charged Bose-gas on a lattice. Such superconductivity differs form the BCS picture in many aspects. This concerns the thermodynamics electromagnetic properties as well as influence of structural disorder.[4,7,9]

Finally, let us relate the present study with the new high-T_c materials. It is now well established that these compounds exhibit quasi-two-dimensional characteristics. This comes from the transport measurements and the band-structure calculations. Our model which is in the present form rather simplified seems to capture some of experimental findings. First of all, superconducting T_c can be high due to the fact that the electron pairing takes place in the whole Brillouin zone contrary to the BCS model. The short coherence length observed in these materials is consistent with the model assuming local short range attractive interaction. The phase diagram derived in this paper containing the SDW ordering and superconductivity is reminisescent of the one observed experimentally in $(\mathrm{La}_{1-x}\mathrm{M}_x)_2\mathrm{CuO}_{4-\delta}$,[36] $M=$Sr,Ba. A fast disappearance of antiferromagnetism in $\mathrm{La}_2\mathrm{CuO}_{4-\delta}$ (Ref. 37) with changing the oxygen vacancies can be interpreted within our model as a consequence of spoiling the Fermi surface nesting. The observed isotope effect in $\mathrm{La}_{2-x}\mathrm{Sr}_x\mathrm{CuO}_{4-\delta}$ (Ref. 38) indicates that superconduc-

[39] R. Micnas, J. Ranninger, and S. Robaszkiewicz, Phys. Rev. B **36**, 4051 (1987).

[40] See, for example, N. Nücker *et al.*, Z. Phys. B **67**, 9 (1987); A. Fujimori *et al.*, Phys. Rev. B **35**, 8814 (1987); P. Steiner *et al.*, Z. Phys. B **67**, 19 (1987); T. Takahashi *et al.*, Phys. Rev. B **36**, 5686 (1987); A. Bianconi *et al.*, Solid State Commun. **63**, 1135 (1987).

[41] Independently electron pairing due to cooperation of superexchange and polaronic effects has been recently considered by Y. Kuramoto and T. Watanabe, Solid State Commun. **63**, 821 (1987).

[42] D. D. Sarma and C. N. R. Rao, J. Phys. C **20**, L659 (1987). R. A. de Groot, H. Gutfreund, and M. Weger, Solid State Commun. **63**, 451 (1987).

[43] J. M. Tranquada, S. M. Heald, and A. R. Moodenbaugh, Phys. Rev. B **36**, 5263 (1987).